

See discussions, stats, and author profiles for this publication at: <https://www.researchgate.net/publication/47498814>

# Differential Reactivity between Two Copper Sites in Peptidylglycine $\alpha$ -Hydroxylating Monooxygenase

ARTICLE in JOURNAL OF THE AMERICAN CHEMICAL SOCIETY · OCTOBER 2010

Impact Factor: 12.11 · DOI: 10.1021/ja103117r · Source: PubMed

---

CITATIONS

15

READS

33

---

## 6 AUTHORS, INCLUDING:



Eduardo E Chufan

U.S. Department of Health and Human Services

41 PUBLICATIONS 742 CITATIONS

[SEE PROFILE](#)



Sean T Prigge

Johns Hopkins Bloomberg School of Public...

64 PUBLICATIONS 2,216 CITATIONS

[SEE PROFILE](#)



Xavier Siebert

Université de Mons

39 PUBLICATIONS 194 CITATIONS

[SEE PROFILE](#)



# NIH Public Access

## Author Manuscript

*J Am Chem Soc.* Author manuscript; available in PMC 2011 November 10.

Published in final edited form as:

*J Am Chem Soc.* 2010 November 10; 132(44): 15565–15572. doi:10.1021/ja103117r.

## Differential Reactivity Between Two Copper Sites in Peptidylglycine $\alpha$ -Hydroxylating Monooxygenase (PHM)

Eduardo E. Chufán<sup>1</sup>, Sean T. Prigge<sup>2</sup>, Xavier Siebert<sup>1</sup>, Betty A. Eipper<sup>3</sup>, Richard E. Mains<sup>3</sup>, and L. Mario Amzel<sup>1,\*</sup>

<sup>1</sup>Department of Biophysics and Biophysical Chemistry, Johns Hopkins School of Medicine, Johns Hopkins University, Baltimore, Maryland 21205, USA

<sup>2</sup>Molecular Microbiology and Immunology, Johns Hopkins Bloomberg School of Public Health, Johns Hopkins University, Baltimore, Maryland 21205, USA

<sup>3</sup>Department of Neuroscience, University of Connecticut Health Center, Farmington, Connecticut 06030, USA

### Abstract

Peptidylglycine  $\alpha$ -Hydroxylating Monooxygenase (PHM) catalyzes the stereospecific hydroxylation of the C $\alpha$  of C-terminal glycine-extended peptides and proteins, the first step in the activation of many peptide hormones, growth factors and neurotransmitters. The crystal structure of the enzyme revealed two non-equivalent Cu sites (Cu<sub>M</sub> and Cu<sub>H</sub>) separated by ~ 11 Å. In the resting state of the enzyme, Cu<sub>M</sub> is coordinated in a distorted tetrahedral geometry by one methionine, two histidines, and a water molecule. The coordination site of the water molecule is the position where external ligands bind. The Cu<sub>H</sub> has a planar T-shaped geometry with three histidines residues and a vacant position that could be potentially occupied by a fourth ligand. Although the catalytic mechanism of PHM and the role of the metals are still being debated, Cu<sub>M</sub> is identified as the metal involved in catalysis while Cu<sub>H</sub> is associated with electron transfer. To further probe the role of the metals, we studied how small molecules such as nitrite (NO<sub>2</sub><sup>-</sup>), azide (N<sub>3</sub><sup>-</sup>) and carbon monoxide (CO) interact with the PHM copper ions. The crystal structure of an oxidized nitrite-soaked PHMcc obtained by 20 hours soaking in mother liquor supplemented with 300 mM NaNO<sub>2</sub>, shows that nitrite anion coordinates Cu<sub>M</sub> in an asymmetric bidentate fashion. Surprisingly, nitrite does *not* bind Cu<sub>H</sub> despite the high concentration used in the experiments (nitrite/protein > 1000). Similarly, azide and carbon monoxide coordinate Cu<sub>M</sub> but not Cu<sub>H</sub> in the PHMcc crystal structures obtained by co-crystallization with 40 mM NaN<sub>3</sub> and by soaking CO under 3 atm of pressure for 30 minutes. This lack of reactivity at the Cu<sub>H</sub> is also observed in the reduced form of the enzyme: CO binds Cu<sub>M</sub> but not Cu<sub>H</sub> in the structure of PHMcc obtained by exposure of a crystal to 3 atm CO for 15 minutes, in the presence of 5 mM ascorbic acid (reductant). The necessity of Cu<sub>H</sub> to maintain its redox potential in a narrow range compatible to its role as an electron-transfer site seems to explain the lack of coordination of small molecules to Cu<sub>H</sub>; coordination of any external ligand will certainly modify its redox potential.

\*To whom correspondence should be addressed, mamzel@jhmi.edu, Phone : (410)955-3955, FAX : (410)955-0637.

### Accession Numbers

Atomic coordinates and structure factors have been submitted to the Protein Data Bank; PDB ID codes are indicated in Tables 1 and 2.

### Supporting Information

Supporting Information Available: Description of the material included. This material is available free of charge via the Internet at <http://pubs.acs.org>.

## Introduction

Many peptides such as hormones, growth factors and neurotransmitters require  $\alpha$ -amidation of their carboxy-terminus to be fully biologically active.<sup>1–3</sup> The  $\alpha$ -amidation is carried out in the trans-Golgi network and in secretory granules of neural and endocrine tissues by two sequential reactions. The first reaction is the stereospecific hydroxylation of the C $\alpha$  of a C-terminal peptidylglycine (see Scheme 1), a reaction catalyzed by Peptidylglycine  $\alpha$ -Hydroxylating Monooxygenase (PHM). The second reaction, an N-dealkylation which yields the amidated peptide and glyoxylate, is catalyzed by Peptidyl- $\alpha$ -hydroxyglycine  $\alpha$ -Amidating Lyase (PAL).<sup>4–5</sup> Although the two enzymes can be expressed and can function independently, in most species they are expressed as a bifunctional single chain enzyme, Peptidylglycine  $\alpha$ -Amidating Monooxygenase (PAM).

PHM is a binuclear copper protein with two non-equivalent type-2 Cu sites, Cu<sub>M</sub> and Cu<sub>H</sub>, separated by 11 Å.<sup>6</sup> It catalyzes the stereospecific C $\alpha$  hydroxylation of the terminal glycine by incorporating one oxygen atom from dioxygen, using ascorbate as the physiological reductant. In the resting state of the enzyme, Cu<sub>M</sub> has a distorted tetrahedral geometry, with one methionine, two histidines, and a water ligand that can be substituted by an external ligand (Figure 1). Cu<sub>H</sub> has a planar T-shaped geometry with three histidines residues and a vacant ligand position that could potentially bind a fourth ligand (Figure 1). Although the chemical structures of the copper centers Cu<sub>M</sub> and Cu<sub>H</sub> are clearly dissimilar, ligand field Magnetic Circular Dichroism (MCD) and Electron Paramagnetic Resonance (EPR) studies on the resting oxidized PHM did not find any measurable differences between the two Cu sites.<sup>7</sup> Interestingly, using nitrite (NO<sub>2</sub><sup>–</sup>) as a metal-ligand, MCD and EPR measurements showed the presence of the two metal centers.<sup>7</sup>

Although the catalytic mechanism of PHM is still being investigated, there is agreement about the main roles of the metals: Cu<sub>M</sub> is the metal involved in catalysis, while Cu<sub>H</sub> is associated with electron transfer.<sup>8–10</sup> As mentioned above, these two copper centers can be classified as type-2 on the basis of their structural and spectroscopic properties: (i) both Cu<sub>M</sub> and Cu<sub>H</sub> are coordinated by histidines (Cu<sub>M</sub> also includes a methionine in its coordination sphere) with a vacant position (Cu<sub>H</sub>) or a position occupied by an exogenous ligand as water (Cu<sub>M</sub>) and (ii) the EPR spectrum show typically a large A value ( $A_z = 157 \times 10^{-4} \text{ cm}^{-1}$ )<sup>7</sup> for the unique copper signal.<sup>11</sup> Further, the two Cu(II) signals of the EPR spectrum of the nitrite-perturbed PHM have large A values ( $A_z = 160 \times 10^{-4} \text{ cm}^{-1}$  and  $165 \times 10^{-4} \text{ cm}^{-1}$ ).<sup>7</sup> Therefore, there is a question about the type-2 characteristics of Cu<sub>H</sub>, which are typical for catalytic sites, and its postulated role as an electron-transfer site. Single electron transfer reactions are usually carried out by type-1 copper centers (blue copper sites), characterized by a cysteine residue coordinated to the copper.<sup>11</sup>

To probe further into the role of the metals and to provide additional insight into the results of the MCD and EPR experiments, we studied how small molecules such as nitrite (NO<sub>2</sub><sup>–</sup>), azide (N<sub>3</sub><sup>–</sup>) and carbon monoxide (CO) interact with the copper active sites. Nitrite is the natural substrate of copper-containing nitrite reductases and thus can bind to biological copper sites.<sup>12</sup> Nitrite also forms metal complexes with Cu(II) adopting different geometries<sup>13–17</sup> and with Cu(I) usually as N-monodentate ligand.<sup>18–19</sup> Azide has also been used as a ligand for copper proteins in the oxidized state<sup>20–22</sup> and there are several examples in the literature of Cu(II) and Cu(I) complexes with azide.<sup>23–24</sup> Carbon monoxide is a well known B-acceptor ligand that can stabilize low oxidation states such as Cu(I) making it a very attractive ligand for reactivity studies of the reduced form of the enzyme. We found that nitrite, azide and carbon monoxide bind Cu<sub>M</sub> but, unexpectedly, do not bind Cu<sub>H</sub> despite the presence of a vacant position in the Cu<sub>H</sub> coordination sphere and the high concentration of the ligands used in the experiments. The lack of coordination of small

molecules thus seems to be an essential feature of the Cu<sub>H</sub> site and is probably related to its proposed functional role as an electron-transfer site.

## Results and Discussion

### ox-PHMcc-nitrite complex

Crystals of the PHMcc-nitrite complex were prepared by soaking protein crystals for 20 hours in mother liquor supplemented with 300 mM NaNO<sub>2</sub>. The 2.35 Å resolution structure revealed that the nitrite anion coordinates Cu<sub>M</sub> in an asymmetric bidentate fashion with copper-to-nitrite oxygen distances of 1.9 Å and 2.6 Å (Figure 2). It displaces the water ligand found in the oxidized form of the enzyme, with one of its oxygens occupying the approximate position of the oxygen of the water molecule. The Cu<sub>M</sub> environment changes significantly from tetracoordinated N<sub>2</sub>(His)S(Met)O<sub>(water)</sub> to pentacoordinated N<sub>2</sub>(His)S(Met)O<sub>2(nitrite)</sub>. This particular coordination mode of a nitrite ligand has been found in nitrite-soaked crystals of nitrite reductases (CuNRs), enzymes for which nitrite is the natural substrate.<sup>25–29</sup> In CuNRs, the catalytic type-2 copper ion is coordinated by three histidine residues, suggesting that the presence of methionine in Cu<sub>M</sub>, at least in the oxidized form of the enzyme, is not playing a critical role in the binding and coordination mode of nitrite. Nitrite has also been found coordinated to the same type-2 Cu of CuNRs as an O-monodentate ligand, but only when substitutions are introduced in residues surrounding the nitrite binding site that render the enzyme inactive.<sup>30</sup> In PHM, the Cu<sub>M</sub> site is open, without any neighboring residue that could force nitrite to adopt a different coordination mode. The PHM structure also revealed that the plane defined by the Cu<sub>M</sub> and the two O atoms of nitrite and the plane defined by the N and the two O atoms of nitrite form a 30 degree angle (Figure S1 in Supporting Information). This feature for Cu-(NO<sub>2</sub>) binding was also observed in several nitrite-soaked CuNRs enzymes.<sup>25</sup> However, small molecule compounds having the Cu-(NO<sub>2</sub>) motif with nitrite bound to Cu as a bidentate ligand, usually exhibit the four atoms (Cu, O<sub>1</sub>, O<sub>2</sub>, N) in the same plane. Out of more than 40 structures deposited in the Cambridge Structural Database (CSD),<sup>31</sup> only 2 have the nitrite bent out of the plane and even in those cases the angle is small (less than 30 degree).<sup>32–33</sup>

Two more nitrite anions were also present in the structure. One is located at a protein-nickel-protein crystal contact,<sup>34</sup> coordinated to Ni(II) in an asymmetric bidentate fashion (Ni-O<sub>nitrite</sub> = 1.95 and 2.65 Å), in a manner similar to that observed in Cu<sub>M</sub>. However, in contrast to what was observed for Cu<sub>M</sub>, the Ni, and the N and two O atoms of nitrite are all in the same plane (Figure S2 in Supporting Information). The other nitrite was found also in the periphery of the protein, hydrogen bonded to the -NH of Gly<sup>258</sup> (2.8 Å) through one of its oxygens.

Remarkably, Cu<sub>H</sub> does not bind nitrite as evidenced by the lack of density at the fourth coordination site of Cu<sub>H</sub> in a 2Fo-Fc electron density map (Figure 2). This is surprising in view that the concentration of nitrite used in the experiments, 300 mM, was very high (nitrite/protein > 1000). Usually, soaking in a 5 mM NaNO<sub>2</sub> solution for 1 hour is enough for binding nitrite to copper(II) in protein crystals.<sup>30</sup> There is clearly something intrinsic to the Cu<sub>H</sub> site structure that prevents nitrite binding despite the presence of a vacant coordination position. Azide was similarly found coordinated to Cu<sub>M</sub> but not Cu<sub>H</sub> in the PHMcc-azide crystal structures (see below).

To enable comparisons between spectroscopic and X-ray structural data, PHMcc-nitrite crystals were prepared using the same concentration of sodium nitrite used in the spectroscopic studies carried out by Solomon and co-workers.<sup>7</sup> Six transitions were observed in the MCD spectrum of nitrite-perturbed PHMcc [ $\sim$  6900 (+),  $\sim$  8900 (-), 10,700

(+), 12,350 (−), 14,200 (+), and 17,000 (−)  $\text{cm}^{-1}$ ], while only two [~12,200 (+) and 16,700 (−)  $\text{cm}^{-1}$ ] are found in the spectrum of the resting PHMcc.7 As the  $\text{Cu}_\text{H}$  site appears unperturbed in the PHMcc-nitrite structure, the new spectroscopic features found for the nitrite-perturbed PHMcc, the absorptions at ~ 6900 (+), ~ 8900 (−), ~ 10,700 (+) and ~ 12,350 (−), must be assigned to the  $\text{Cu}_\text{M}(\text{NO}_2)$  site of the enzyme. The  $\text{Cu}_\text{M}^{2+}$  is in a five-coordinate environment with two histidines, one methionine and nitrite acting as an asymmetric bidentate ligand. The stereochemistry around the copper(II) ion is best described as a distorted square-pyramidal geometry (SPY) rather than trigonal bipyramidal (TBPY). The geometric parameter  $\tau = (\beta - \alpha)/60$  (where  $\beta$  and  $\alpha$  are the largest basal angles;  $\tau = 0$  corresponds to a perfect SPY while  $\tau = 1$  indicates a perfect TBPY) is used to characterize the stereochemistry around the  $\text{Cu}_\text{M}^{2+}$  ion.<sup>35</sup> The basal plane is defined by the  $\text{N}_{\text{His}242^-}\text{S}_{\text{Met}}\text{O}_1\text{nitrite-O}_2\text{nitrite}$ , where the largest angles are  $\text{S-Cu-O}_1 = 152^\circ$  ( $\beta$ ) and  $\text{N-Cu-O}_2 = 139^\circ$  ( $\alpha$ ). Thus, the value of  $\tau = 0.22$  indicates a geometry for  $\text{Cu}_\text{M}$  better described as a distorted square-pyramid (SPY). The apical position is occupied by the  $\text{N}\varepsilon$  donor of His<sup>244</sup>. It is interesting to note that all four possible copper(II) d-d transitions are observed in the MCD spectrum of PHM for  $\text{Cu}_\text{M}$  when it is coordinated by nitrite. Spectral assignments to specific orbital transitions require a more detail ligand field analysis which is beyond the scope of the present work. The difference between the 14,200 (+) (nitrite-perturbed) MCD absorption band assigned to  $\text{Cu}_\text{H}$  and the band at ~12,200 (+) (native) could be due to the noticeable broadness of the band and the fact that the native ~12,200 (+) band is formed by contributions of both  $\text{Cu}_\text{H}$  and  $\text{Cu}_\text{M}$  electronic transitions. Also, binding of ligand to  $\text{Cu}_\text{M}$  produces in most cases small but significant changes in the histidines coordinating  $\text{Cu}_\text{H}$ . These involve mainly changes in the conformations of the coordinating histidines in the form of changes in  $\chi_2$  but sometimes also in  $\chi_1$ . These changes are sometimes as large as 90 degrees. This type of changes will affect in a direct and significant way the interactions between the metal orbitals and those of the ligands and may result in significant spectral changes.

Further spectroscopic characterization was provided by X-band EPR studies.<sup>7</sup> The spectrum of PHM shows only one set of Cu(II) hyperfine couplings ( $g_x=2.050$ ,  $g_y=2.060$ ,  $g_z=2.288$ ) making it impossible to distinguish  $\text{Cu}_\text{M}$  from  $\text{Cu}_\text{H}$ . The nitrite-PHMcc on the other hand shows two sets of Cu(II) hyperfine couplings in the  $g_z$  region (2.265 and 2.298), thus distinguishing the two copper sites. The features at  $g_x=2.060$ ,  $g_y=2.060$ ,  $g_z=2.265$  can be assigned to the  $\text{Cu}_\text{M}^{\text{II}}(\text{NO}_2)$  site while the ones at  $g_x=2.060$ ,  $g_y=2.060$ ,  $g_z=2.298$  to the  $\text{Cu}_\text{H}$ , because only the  $\text{Cu}_\text{H}$  was found unperturbed with respect to the native enzyme. The distorted square pyramidal geometry found for  $\text{Cu}_\text{M}(\text{NO}_2)$  is consistent with the EPR spectrum ( $g_z > g_x, g_y > 2.0$ ) which clearly shows that the ground state orbital for the  $\text{Cu}_\text{M}^{2+}$  unpaired electron is  $d(x^2-y^2)$ .

### ox-PHMcc-azide complex

PHMcc crystals soaked in mother liquor supplemented with 350 mM  $\text{NaN}_3$ , the azide concentration used in the spectroscopic studies of Solomon and co-workers,<sup>7</sup> were seriously damaged after one hour and completely dissolved a few hours later. Crystals soaked for one hour were tested for X-ray diffraction but the resolution of the data was very low ( $> 3.5 \text{ \AA}$ ). Crystals that diffracted to an acceptable resolution were prepared by co-crystallization using 40 mM  $\text{NaN}_3$ . Final co-crystallization conditions were 0.5 mM  $\text{CuSO}_4$ , 1.25 mM  $\text{NiCl}_2$ , 100 mM sodium cacodylate pH = 5.5, 5% glycerol, and 40 mM  $\text{NaN}_3$ , at room temperature. After 11 days, data were collected from a crystal that diffracted to 2.4  $\text{\AA}$  resolution. The structure determined using these data revealed an azide anion coordinated to the  $\text{Cu}_\text{M}$  ( $\text{Cu-N} = 2.0 \text{ \AA}$ ), replacing the water ligand found in the oxidized state of the native enzyme, or the  $\text{O}_2$  bound in the reduced form in the presence of substrate, and keeping the same tetrahedral geometry around copper. Kinetic and spectroscopic studies of azide binding to dopamine  $\beta$ -

hydroxylase (DBH), a tetrameric PHM analog, were interpreted as indicating that azide binds to a single copper per monomer, in agreement with the crystallographic data on PHM.  
36

Electron density maps also showed a sodium ion bound to the azide ligand, behaving as a  $\mu(1,1)$  bridging bidentate ligand connecting the  $\text{Cu}_M^{2+}$  to the  $\text{Na}^+$  (Figure 3). This  $\text{Cu}^{2+}$ - $(\text{N}_3^-)$ - $\text{Na}^+$  motif has not been previously observed in proteins and is very rare even in synthetic metal complexes.<sup>37</sup> In addition, the loop Asp<sup>127</sup>-Glu<sup>128</sup>-Gly<sup>129</sup>-Thr<sup>130</sup> moves closer to the  $\text{Cu}_M$  site, in comparison to the free enzyme (Figure 4). The sodium ion binds to the azide, attracts the carboxylate groups of the Asp<sup>127</sup> and Glu<sup>128</sup>, and changes the conformation of the loop. The residues flanking the loop Cys<sup>126</sup> and Cys<sup>131</sup> are held by disulfide bridges to Cys<sup>81</sup> and Cys<sup>114</sup>, respectively, preventing a large-scale propagation of the new conformation. However, this loop is not moved in PHMcc-azide crystals obtained by soaking (see Supporting Information), suggesting that this conformational change cannot take place within the native crystals upon binding of azide to the  $\text{Cu}_M$  site.

The coordination of the  $\text{Cu}_H$  site in the structure of the PHMcc-azide crystal is also intriguing. In the free enzyme,  $\text{Cu}_H$  has a vacant coordination site that could potentially be occupied by a fourth ligand. However,  $\text{Cu}_H$  does not bind azide (Figure 3). This is true not only in the co-crystallized sample at lower azide concentration. Despite the low resolution (3.0 to 3.3 Å) of the X-ray datasets obtained in soaking experiments at (i) 100 mM  $\text{NaN}_3$  for 1.5 hours, (ii) 50 mM  $\text{NaN}_3$  for 26 hours and (iii) 50 mM  $\text{NaN}_3$  for 6 hours, the structures of these crystals all revealed azide bound to  $\text{Cu}_M$  but not to  $\text{Cu}_H$  (see Table 1 and Supporting Information), consistent with the observations in the higher resolution structure obtained by co-crystallization. Further, the high B factor exhibited for  $\text{Cu}_H$  in all datasets (80–105 Å<sup>2</sup>) in comparison to the protein average B factor (50 Å<sup>2</sup>) may be indicative of an occupancy lower than 1.0, suggesting that azide may remove  $\text{Cu}_H$  after long exposure of crystals to high  $\text{NaN}_3$  concentration.

Differences observed between the X-ray structures of PHMcc-azide complexes determined here and the published spectroscopic data (MCD, EPR) obtained on PHMcc solution with 350 mM  $\text{NaN}_3$ ,<sup>7</sup> may be a consequence of the different  $\text{NaN}_3$  concentration used in the experiments.

### red-PHMcc-CO complex

The ability of metal ions to bind ligands and stabilize their coordination sphere depends, among other factors, on their oxidation state. Both copper ions in PHM alternate between Cu(II) and Cu(I) in the catalytic cycle.<sup>38</sup> Thus, the behavior of reduced PHM in the presence of carbon monoxide – a very good ligand for copper(I) – was investigated (see Table 2 for crystallographic data). A PHMcc crystal in 5 mM ascorbic acid was exposed to 3 atm CO for 15 minutes and then analyzed by X-ray crystallography (see experimental section for further details). The structure shows CO bound to  $\text{Cu}_M$  as an “end-on, bent” ligand; Cu-C distance is 1.8 Å and  $\text{Cu}_M$ -C-O angle is 110° (Figure 5). This geometry is the same geometry adopted by dioxygen in the precatalytic intermediate formed by soaking PHMcc crystals with slow substrate and ascorbate in the presence of dioxygen.<sup>34</sup> Again, no electron density is found at the open coordination position of  $\text{Cu}_H$ , indicating that  $\text{Cu}(I)_H$  is not reactive against carbon monoxide. A water molecule is found interacting very weakly with the  $\text{Cu}_H$  ( $\text{Cu}_H$ -O<sub>water</sub> = 3.3 Å, not shown in Figure 5). The lack of binding of CO at the  $\text{Cu}_H$  site is consistent with the lack of reactivity against molecular oxygen observed for the precatalytic intermediate of PHMcc (see above). In the final refinement,  $\text{Cu}_H$  refined to an occupancy of 0.7, a fact that reflects that part of the  $\text{Cu}_H$  is displaced under the conditions of the experiment. Binding of CO to  $\text{Cu}_M$  and the lack of reactivity of  $\text{Cu}_H$  is fully consistent

with the previous results of EXAFS and FTIR studies<sup>39</sup> as well as with studies of DBH, a PHM analog.<sup>40-41</sup>

### ox-PHMcc-CO complex

Although CO is not as good a ligand for Cu(II) as for Cu(I), CO-soaking experiments were carried out with the oxidized form of the enzyme to further probe the reactivity of Cu(II)<sub>H</sub> and to compare it with the structure of the reduced PHMcc-CO. The structure revealed that CO coordinates Cu(II)<sub>M</sub> with the same geometry observed in the complex with the reduced form of the enzyme. However, in addition to its regular conformation, the loop spanning residues 127–130 is found also in an alternative conformation (occupancy=0.5), similar to that found in the ox-PHMcc-azide structure obtained by co-crystallization (see above). In the CO case, the carboxylate of Glu<sup>128</sup> of the new conformation coordinates Cu<sub>M</sub> as a monodentate ligand. Even though pressure unfolding usually requires much higher pressures (e.g. on the order of 10,000 psi)<sup>42</sup> than that used in these investigations (50 psi), one tentative explanation for this double conformation is that it was caused by pressure.

### red-PHMcc-nitrite and red-PHMcc-azide complexes

The behavior of reduced PHM in the presence of high concentrations of nitrite and azide was also investigated (see Table 2 for crystallographic data). As in the oxidized state of the enzyme, nitrite and azide bind Cu(I)<sub>M</sub> (Figure S4 in Supporting Information). Surprisingly, Cu(I)<sub>H</sub> is completely removed from its site in the presence of the high concentrations of nitrite or azide (300 mM NaNO<sub>2</sub> or 40 mM NaN<sub>3</sub>). Also, in the azide complex, the Cu(I)<sub>M</sub> site is only partially occupied; the structure was refined with half occupancy for the Cu(I)<sub>M</sub>-azide moiety. The low resolution of these crystals (> 3 Å) in comparison with the typical resolution of reduced PHM crystals (around 2 Å) is probably related to structural deterioration caused by the loss of Cu<sub>H</sub>.

### Binding experiments in the presence of substrate

We carried out experiments to investigate whether the presence of substrate has any effect at the copper centers that could modify their chemical behavior towards molecules such as nitrite or azide. Our experiments had to be carried out in the oxidized state of the enzyme because Cu<sub>H</sub> is removed from the protein in the reduced state (see above). Using the substrate (N-*a*-acetyl-3,5-diiodotyrosylglycine, Ac-DiI-YG) and the experimental conditions reported previously,<sup>8,43</sup> crystals of PHM-substrate were prepared by soaking for one hour native crystals of PHMcc in mother liquor (ML) supplemented with 1 mM substrate, followed by soaking in ML supplemented with 1 mM substrate and sodium nitrite or sodium azide (see Table 1 for crystallographic data). The X-ray structures did not show bound substrate in either case but, as found in the experiments without substrate, Cu<sub>M</sub> binds nitrite or azide while Cu<sub>H</sub> did not (Figure S5 in Supporting Information). Binding of nitrite or azide and/or high concentration of sodium nitrite or sodium azide in the media seem to prevent substrate binding to PHM.

### Why does Cu<sub>H</sub> NOT bind small molecules?

We have shown that under the conditions used azide, nitrite and carbon monoxide do not bind to Cu<sub>H</sub>. We have previously shown that Cu<sub>H</sub> does not bind dioxygen under conditions in which it binds to Cu<sub>M</sub>. Blackburn and coworkers showed that isocyanides bind to Cu<sub>M</sub> but not to Cu<sub>H</sub>.<sup>44</sup> They also showed that in DBH, CO binds to a single copper per monomer.<sup>40</sup> All these results point to Cu<sub>H</sub> as a metal site with unusual reactivity.

The catalytic  $\alpha$ -hydroxylation reaction uses dioxygen as the oxygen source. The two electrons required for the dioxygen reduction are provided by ascorbate via one-electron

reduction of Cu<sub>M</sub> and Cu<sub>H</sub>. In this manner, PHM starts its catalytic cycle in the Cu<sup>I</sup><sub>M</sub>...Cu<sup>I</sup><sub>H</sub> stage. The substrate binds close to the Cu<sub>M</sub> site and a reactive oxygen species bound to Cu<sub>M</sub> is responsible for substrate hydrogen abstraction. In this scenario, Cu<sub>H</sub> is an electron-transfer site, providing the second electron required to complete the catalytic cycle. The driving force for this step is given by the difference in redox potential between Cu<sub>H</sub> and that of the acceptor species, which includes an oxygen-bound Cu<sub>M</sub>. The lack of coordination of small molecules to Cu<sub>H</sub> is probably related to the necessity for Cu<sub>H</sub> to maintain its redox potential in a narrow range to maintain its function as an electron donor. It is known that alterations in the coordination sphere (number and type of ligand donor atoms) and stereochemistry at the metal center can produce great differences in the potential at which electron-transfer reactions occur.<sup>45</sup> The change from three histidines T-shape geometry to, for instance, three histidines and one small ligand (e.g. monodentate nitrite, azide or carbon monoxide) square planar geometry would surely change Cu(I)/(II)<sub>H</sub> redox potential. Were this site accessible to small molecule binding, metabolites present in the physiological environment would change the enzyme kinetics.

Binding of O<sub>2</sub> to Cu(I)<sub>H</sub> would be particularly detrimental as it could be reduced to superoxide and released. The X-ray structure of reduced PHMcc with dioxygen bound to the Cu<sub>M</sub> in the presence of a slow-substrate, revealed that Cu<sub>H</sub> does not bind dioxygen.<sup>34</sup> This is essentially the same reactivity we observe with carbon monoxide. These results are consistent with the proposal presented here: the architecture of the Cu<sub>H</sub> site prevents small molecule binding to avoid any redox potential change.

From a chemical point of view it is very difficult to understand why very good copper ligands such as nitrite, azide or carbon monoxide do not bind Cu<sub>H</sub>, since there is a vacant position on its coordination sphere. Apparently the bis-histidines His<sup>107</sup>-His<sup>108</sup>, in concert with His<sup>172</sup> -all three histidines binding through the Nδ donor- form a particular geometry and electronic structure for Cu<sub>H</sub> that prevents binding at the fourth vacant position. One characteristic of the Cu<sub>H</sub> coordination that may account for its lack of reactivity is its unusual geometry: the three histidines are in a shape that we described in general as a T-configuration. However, the coordination of Cu<sub>H</sub> is more unusual than that. The three His-Cu-His angles in the 13 complexes (10 reported in this manuscript) are the following: H<sup>107</sup>-Cu<sub>H</sub>-H<sup>108</sup> ranges between 138.6 and 151.4 degrees; H<sup>107</sup>-Cu<sub>H</sub>-H<sup>172</sup> between 107.2 and 111.9; and H<sup>108</sup>-Cu<sub>H</sub>-H<sup>172</sup> between 94.3 and 110.9. This arrangement is somewhere between a square planar with one empty position and a planar trigonal. It is possible that this coordination, imposed by the protein environment, prevents binding to a fourth site. In addition, in all three cases the histidines coordinate the copper with their Nδ the most positionally restricted of the two histidine nitrogens, making it more difficult for the coordination to rearrange to accommodate a fourth ligand. A detailed quantum mechanical analysis of Cu<sub>H</sub> could provide insights on this matter.

The metal coordination in outer-sphere electron-transfer sites is found fully occupied with ligands provided by the protein structure. Type-1 copper sites in blue copper proteins, which almost exclusively function as electron-transfer molecules, are coordinated by two His and one Cys in a distorted trigonal plane with an axial protein residue (usually Met) in an overall distorted tetrahedral geometry; no vacant/open position is present in their coordination sphere.<sup>46-47</sup> The binuclear Cu<sub>A</sub> center as in cytochrome *c* oxidase is another example.<sup>48</sup> Recently, a red copper protein with a copper site with an open position in the reduced form (a water molecule occupies that position in the oxidized form) has been spectroscopically and structurally characterized.<sup>49-50</sup> It had been proposed that this red copper protein (absorption band at 390 nm), isolated from *Nitrosomonas europaea*, might be involved in electron-transfer because it shares significant sequence homology to blue copper proteins

and has a typical Cu-thiolate bond. However, later investigations suggest that electron-transfer is accomplished by an inner-sphere mechanism.<sup>51</sup>

The same feature (absence of an open coordination position) is observed for iron electron-transfer proteins that work via an outer-sphere mechanism. From the simple tetrahedral iron-sulfur center such as is found in rubredoxin to the very complex iron-sulfur clusters as in other ferredoxins,<sup>52</sup> and even the six-coordinated heme in cytochromes,<sup>53</sup> in all cases, efficient outer-sphere electron-transfer is guaranteed with a fully saturated coordination sphere for the metal site. The only exception is the heme at cytochrome *c'* which has an open coordination position at the active site;<sup>54</sup> however its physiological role as an electron-transfer site is still unclear.<sup>55–56</sup>

In summary, all very well known outer-sphere electron-transfer metal-sites have the attribute to be fully saturated in their coordination sphere by ligands provided by the protein structure. Surprisingly, the Cu<sub>H</sub> outer-sphere electron-transfer site in PHM has an apparent open coordination position that remains empty at high concentrations of small anions/molecules such as nitrite, azide and carbon monoxide. Something essential with the typical architecture of Cu<sub>H</sub> creates an electronic structure for Cu<sub>H</sub> that impedes the binding of an extra-ligand. This property ensures Cu<sub>H</sub> maintains its redox potential in a narrow range compatible to its role as an efficient electron-transfer in the catalytic cycle of PHM.

## Experimental Section

### Preparation of crystals and soaking experiments

Stably transfected Chinese Hamster Ovary (CHO) cell lines secreting PHMcc (residues 42 to 356) were constructed using the pcIS vector system<sup>57</sup> and purified as described previously.<sup>6</sup> The native protein was crystallized by the hanging-drop diffusion method at 293 K. Thus, PHMcc (1 μl; concentration = 16 mg/ml) was mixed with an equal volume of mother liquor (0.1–0.5 mM CuSO<sub>4</sub>, 1.0–1.25 mM NiCl<sub>2</sub>, 100 mM sodium cacodylate pH = 5.5, 3.08 mM NaN<sub>3</sub>, 5% glycerol) and crystals appeared in 3–4 days. As reported before, nickel(II) ion is incorporated into PHMcc structure as a crystal contact site.

### Oxidized PHMcc-nitrite crystals

Nitrite-soaked PHMcc crystals were obtained by placing native PHMcc crystals in mother liquor supplemented with 300 mM NaNO<sub>2</sub> for 20 hours at room temperature. The crystals were then transferred to fresh mother liquor supplemented with 300 mM NaNO<sub>2</sub> and 30 % glycerol as a cryo-protectant, prior to flash-freezing. Data collection and refinement statistics are reported in Table 1.

### Oxidized PHMcc-azide crystals

ox-PHM-azide crystals were obtained by co-crystallization at 293 K, using the same methodology as for crystallizing native PHMcc but the mother liquor contained 40 mM NaN<sub>3</sub> instead of 3.08 mM. Crystals appear in 3–4 days.

### Oxidized PHMcc-CO crystals

A pressure chamber built by Kas Kumar was used for CO soaking into PHM (unpublished work). The reservoir of the pressure chamber was filled with mother liquor containing 25% of glycerol and saturated with CO. Native PHMcc crystals were soaked into the CO-containing cryoprotectant solution for less than a minute and transferred with a loop to the pressure chamber. The chamber was purged several times with low pressure of CO, then gradually filled with 50 psi CO and finally maintained at this pressure during 30 minutes.

After bringing back the chamber to atmospheric pressure, the crystal was rapidly removed and cryo-frozen in liquid nitrogen.

### Oxidized PHMcc-nitrite crystals in the presence of substrate

PHMcc crystals, grown as described above, were first soaked in mother liquor supplemented with 1 mM substrate (Ac-3,5-diL-YG) for 1 hour at room temperature. Then the crystals were soaked in a solution containing 300 mM NaNO<sub>2</sub>, 1 mM substrate and the rest of the mother liquor components, for 14 hours at room temperature.

### Oxidized PHMcc-azide crystals in the presence of substrate

Crystals of PHMcc complexed with substrate were obtained as described above (1 hour soaking in mother liquor with 1 mM substrate). Then the crystals were soaked in a solution containing 40 mM NaN<sub>3</sub>, 1 mM substrate and the rest of the mother liquor components, for 8 hours at room temperature.

### Reduced PHMcc-CO crystals

Reduced CO-soaked PHMcc crystals were prepared following the same pressure chamber and protocol described for the oxidized CO-soaked PHMcc crystals (see above) but adding 5 mM ascorbic acid to the cryoprotectant solution and the crystal was in the pressure chamber filled with 50 psi CO for 15 minutes.

### Reduced PHMcc-nitrite crystals

PHMcc crystals, grown as described above, were reduced with ascorbic acid by soaking native crystals for 1 hour in mother liquor with 5 mM ascorbic acid (1.85 mM NiCl<sub>2</sub>, 100 mM sodium cacodylate pH = 5.5, 3.08 mM NaN<sub>3</sub>, 5% glycerol). The reduced crystals were then soaked in a solution containing 300 mM NaNO<sub>2</sub>, 5 mM ascorbic acid and the rest of the mother liquor components, for 13 hours at room temperature.

### Reduced PHMcc-azide crystals

Reduced PHMcc crystals were obtained as described above, then soaked in a solution containing 40 mM NaN<sub>3</sub>, 5 mM ascorbic acid in mother liquor components, for 6 hours at room temperature.

### Data collection, structures determination and refinement

Diffraction data were collected on single frozen crystals, either at a home source (Rigaku RU-200 rotating anode and R-AXIS IV image plate detector) or at beamline X6A, X4C or X25 of the National Synchrotron Light Source at Brookhaven National Laboratory. Frames were processed with HKL2000 software package.<sup>58</sup> All crystals belong to the orthorhombic space group *P*2<sub>1</sub>2<sub>1</sub>2<sub>1</sub>. All structures were determined by molecular replacement with the program AMoRe<sup>59</sup> using the coordinates of the native enzyme (1PHM.pdb) as the search model. The models were built interactively with program O<sup>60</sup> and refined using REFMAC 5.0 as implemented in CCP4 suite programs.<sup>61–62</sup> Anisotropic refinement using translation, libration and screw rotation (TLS) of rigid bodies was carried out using four groups (residues 46–65; 66–185; 186–302 and 303–354) or each domain (46–197 and 198–354) as TLS group.<sup>63–64</sup> Solvent molecules were added automatically using program ARP/WARP<sup>62–65</sup> and visually inspected with program O.<sup>60</sup> Refinement was monitored by calculating R<sub>free</sub> values using 5% of the reflections set aside for cross-validation. Crystallographic data collection and refinement statistics are summarized in Tables 1 and 2.

## Supplementary Material

Refer to Web version on PubMed Central for supplementary material.

## Acknowledgments

Mario Bianchet and the staff at beamlines X6A, X4C and X25 of the National Synchrotron Light Source, Brookhaven National Laboratory, are gratefully acknowledged for assistance during synchrotron data collection. This work was supported by a National Science Foundation grant MCB-0450465 (L.M.A. and S.T.P.) and National Institutes of Health grant DK032949 (E.A.E.).

## References

1. Eipper BA, Stoffers DA, Mains RE. *Annu Rev Neurosci*. 1992; 15:57. [PubMed: 1575450]
2. Merkler DJ. *Enzyme Microb Technol*. 1994; 16:450. [PubMed: 7764886]
3. Prigge ST, Mains RE, Eipper BA, Amzel LM. *Cellular and Molecular Life Sciences*. 2000; 57:1236. [PubMed: 11028916]
4. Kolhekar AS, Bell J, Shiozaki EN, Jin L, Keutmann HT, Hand TA, Mains RE, Eipper BA. *Biochemistry-US*. 2002; 41:12384.
5. Chufan EE, De M, Eipper BA, Mains RE, Amzel LM. *Structure*. 2009; 17:965. [PubMed: 19604476]
6. Prigge ST, Kolhekar AS, Eipper BA, Mains RE, Amzel LM. *Science*. 1997; 278:1300. [PubMed: 9360928]
7. Chen P, Bell J, Eipper BA, Solomon EI. *Biochemistry-US*. 2004; 43:5735.
8. Prigge ST, Kolhekar AS, Eipper BA, Mains RE, Amzel LM. *Nat Struct Biol*. 1999; 6:976. [PubMed: 10504734]
9. Klinman JP. *J Biol Chem*. 2006; 281:3013. [PubMed: 16301310]
10. Crespo A, Martí MA, Roitberg AE, Amzel LM, Estrin DA. *J Am Chem Soc*. 2006; 128:12817. [PubMed: 17002377]
11. Wijma HJ, MacPherson I, Farver O, Tocheva EI, Pecht I, Verbeet MP, Murphy ME, Canters GW. *J Am Chem Soc*. 2007; 129:519. [PubMed: 17227014]
12. MacPherson IS, Murphy MEP. *Cellular and Molecular Life Sciences*. 2007; 64:2887. [PubMed: 17876515]
13. Lehnert N, Cornelissen U, Neese F, Ono T, Noguchi Y, Okamoto K, Fujisawa K. *Inorganic Chemistry*. 2007; 46:3916. [PubMed: 17447754]
14. Karlin, KD.; Tyeklár, Z. *Bioinorganic chemistry of copper*. New York: Chapman & Hall; 1993.
15. Tolman WB. *Inorganic Chemistry*. 1991; 30:4877.
16. Ruggiero CE, Carrier SM, Tolman WB. *Angew Chem Int Edit*. 1994; 33:895.
17. Walsh A, Walsh B, Murphy B, Hathaway BJ. *Acta Crystallogr B*. 1981; 37:1512.
18. Kujime M, Izumi C, Tomura M, Hada M, Fujii H. *Journal of the American Chemical Society*. 2008; 130:6088. [PubMed: 18412340]
19. Halfen JA, Mahapatra S, Wilkinson EC, Gengenbach A, Young VG Jr, Que L, Tolman WB. *J Am. Chem. Soc.* 1996; 118:763.
20. Tocheva EI, Eltis LD, Murphy MEP. *Biochemistry-US*. 2008; 47:4452.
21. Rogers MS, Tyler EM, Akyumani N, Kurtis CR, Spooner RK, Deacon SE, Tamber S, Firbank SJ, Mahmoud K, Knowles PF, Phillips SEV, McPherson MJ, Dooley DM. *Biochemistry-US*. 2007; 46:4606.
22. Tsai LC, Bonander N, Harata K, Karlsson G, Vanngard T, Langer V, Sjolin L. *Acta Crystallogr D*. 1996; 52:950. [PubMed: 15299604]
23. Casella L, Gullotti M, Pallanza G, Buga M. *Inorganic Chemistry*. 1991; 30:221.
24. Pettinari C. *Polyhedron*. 2001; 20:2755.
25. Tocheva EI, Rosell FI, Mauk AG, Murphy ME. *Science*. 2004; 304:867. [PubMed: 15131305]
26. Dodd FE, Van Beeumen J, Eady RR, Hasnain SS. *J Mol Biol*. 1998; 282:369. [PubMed: 9735294]

27. Murphy MEP, Turley S, Adman ET. *Journal of Biological Chemistry*. 1997; 272:28455. [PubMed: 9353305]
28. Antonyuk SV, Strange RW, Sawers G, Eady RR, Hasnain SS. *Proc Natl Acad Sci U S A*. 2005; 102:12041. [PubMed: 16093314]
29. Jacobson F, Pistorius A, Farkas D, De Grip W, Hansson O, Sjolin L, Neutze R. *J Biol Chem*. 2007; 282:6347. [PubMed: 17148448]
30. Boulanger MJ, Murphy ME. *Protein Sci*. 2003; 12:248. [PubMed: 12538888]
31. Allen FH. *Acta Crystallogr B*. 2002; 58:380. [PubMed: 12037359]
32. Chattopadhyay S, Drew MGB, Ghosh A. *Inorg Chim Acta*. 2006; 359:4519.
33. Shim YB, Choi SN, Lee SJ, Kang SK, Lee YM. *Acta Crystallogr E*. 2004; 60:M1573.
34. Prigge ST, Eipper BA, Mains RE, Amzel LM. *Science (Washington, DC, United States)*. 2004; 304:864.
35. Addison AW, Rao TN, Reedijk J, van Rijn J, Verschoor GC. *J. Chem. Soc. Dalton Trans*. 1984:1349.
36. Blackburn NJ, Collison D, Sutton J, Mabbs FE. *Biochem J*. 1984; 220:447. [PubMed: 6331417]
37. Goher MAS, Mautner FA. *Polyhedron*. 1995; 14:1439.
38. Freeman JC, Villafranca JJ, Merkler DJ. *J. Am. Chem. Soc*. 1993; 115:4923.
39. Jaron S, Blackburn NJ. *Biochemistry-US*. 1999; 38:15086.
40. Blackburn NJ, Pettingill TM, Seagraves KS, Shigeta RT. *J Biol Chem*. 1990; 265:15383. [PubMed: 2394729]
41. Pettingill TM, Strange RW, Blackburn NJ. *J Biol Chem*. 1991; 266:16996. [PubMed: 1894598]
42. Panick G, Malessa R, Winter R, Rapp G, Frye KJ, Royer CA. *Journal of Molecular Biology*. 1998; 275:389. [PubMed: 9466917]
43. Siebert, XPhD. Johns Hopkins School of Medicine. 2005
44. Rhames FC, Murthy NN, Karlin KD, Blackburn NJ. *J Biol Inorg Chem*. 2001; 6:567. [PubMed: 11472020]
45. Lippard, SJ.; Berg, JM. *Principles of bioinorganic chemistry*. Mill Valley, Calif: University Science Books; 1994.
46. Solomon EI, Szilagyi RK, DeBeer George S, Basumallick L. *Chem Rev*. 2004; 104:419. [PubMed: 14871131]
47. Sakurai T, Kataoka K. *Cell Mol Life Sci*. 2007; 64:2642. [PubMed: 17639274]
48. Kim E, Chufan EE, Kamaraj K, Karlin KD. *Chemical Reviews (Washington, DC, United States)*. 2004; 104:1077.
49. Basumallick L, Sarangi R, DeBeer George S, Elmore B, Hooper AB, Hedman B, Hodgson KO, Solomon EI. *J Am Chem Soc*. 2005; 127:3531. [PubMed: 15755175]
50. Lieberman RL, Arciero DM, Hooper AB, Rosenzweig AC. *Biochemistry-US*. 2001; 40:5674.
51. Solomon EI. *Inorg Chem*. 2006; 45:8012. [PubMed: 16999398]
52. Venkateswara Rao P, Holm RH. *Chem Rev*. 2004; 104:527. [PubMed: 14871134]
53. Walker FA. *Chem Rev*. 2004; 104:589. [PubMed: 14871136]
54. Benini S, Rypniewski WR, Wilson KS, Ciurli S. *J Inorg Biochem*. 2008; 102:1322. [PubMed: 18295896]
55. Meyer TE, Cheddar G, Bartsch RG, Getzoff ED, Cusanovich MA, Tollin G. *Biochemistry-US*. 1986; 25:1383.
56. Mayburd AL, Kassner RJ. *Biochemistry-US*. 2002; 41:11582.
57. Kolhekar AS, Keutmann HT, Mains RE, Quon AS, Eipper BA. *Biochemistry-US*. 1997; 36:10901.
58. Otwinowski Z, Minor W. *Methods in Enzymology*. 1997; 276:307.
59. Navaza J. *Acta Crystallogr D Biol Crystallogr*. 2001; 57:1367. [PubMed: 11567147]
60. Jones TA, Kjeldgaard M. *Methods Enzymol*. 1997; 277:173. [PubMed: 18488310]
61. Murshudov GN, Vagin AA, Dodson EJ. *Acta Crystallogr D Biol Crystallogr*. 1997; 53:240. [PubMed: 15299926]
62. *Acta Crystallogr D Biol Crystallogr*. 1994; 50:760. [PubMed: 15299374]

63. Painter J, Merritt EA. *J Appl Crystallogr.* 2006; 39:109.
64. Winn MD, Murshudov GN, Papiz MZ. *Methods Enzymol.* 2003; 374:300. [PubMed: 14696379]
65. Lamzin VS, Wilson KS. *Method Enzymol.* 1997; 277:269.

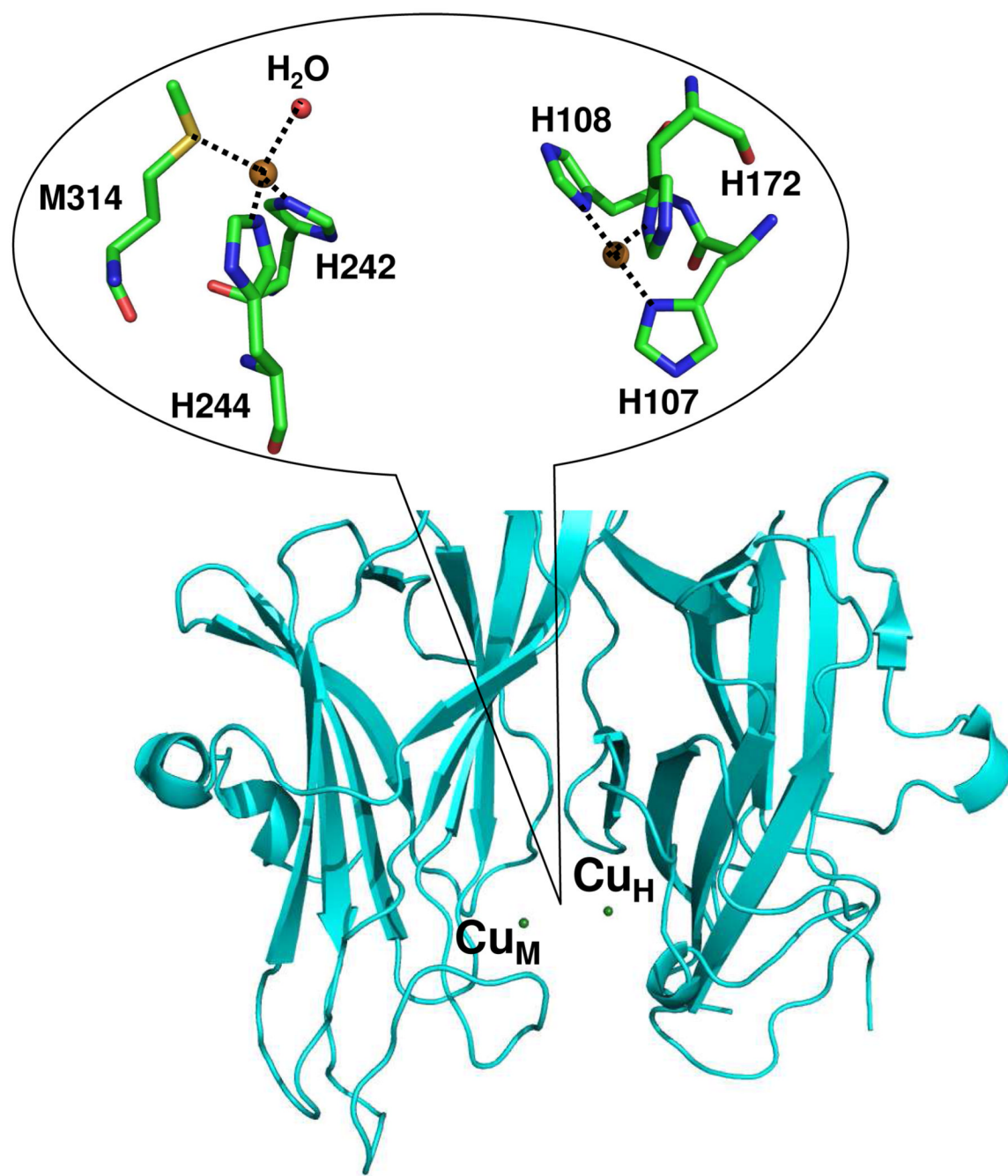


**Figure 1. The structure of  $\text{Cu}_M$  and  $\text{Cu}_H$  sites of PHMcc**

$\text{Cu}_M$  is the catalytic site and  $\text{Cu}_H$  is the electron-transfer site. The two copper centers are separated 11 Å by an inter-domain cleft fully accessible to substrates, solvent and small molecules.

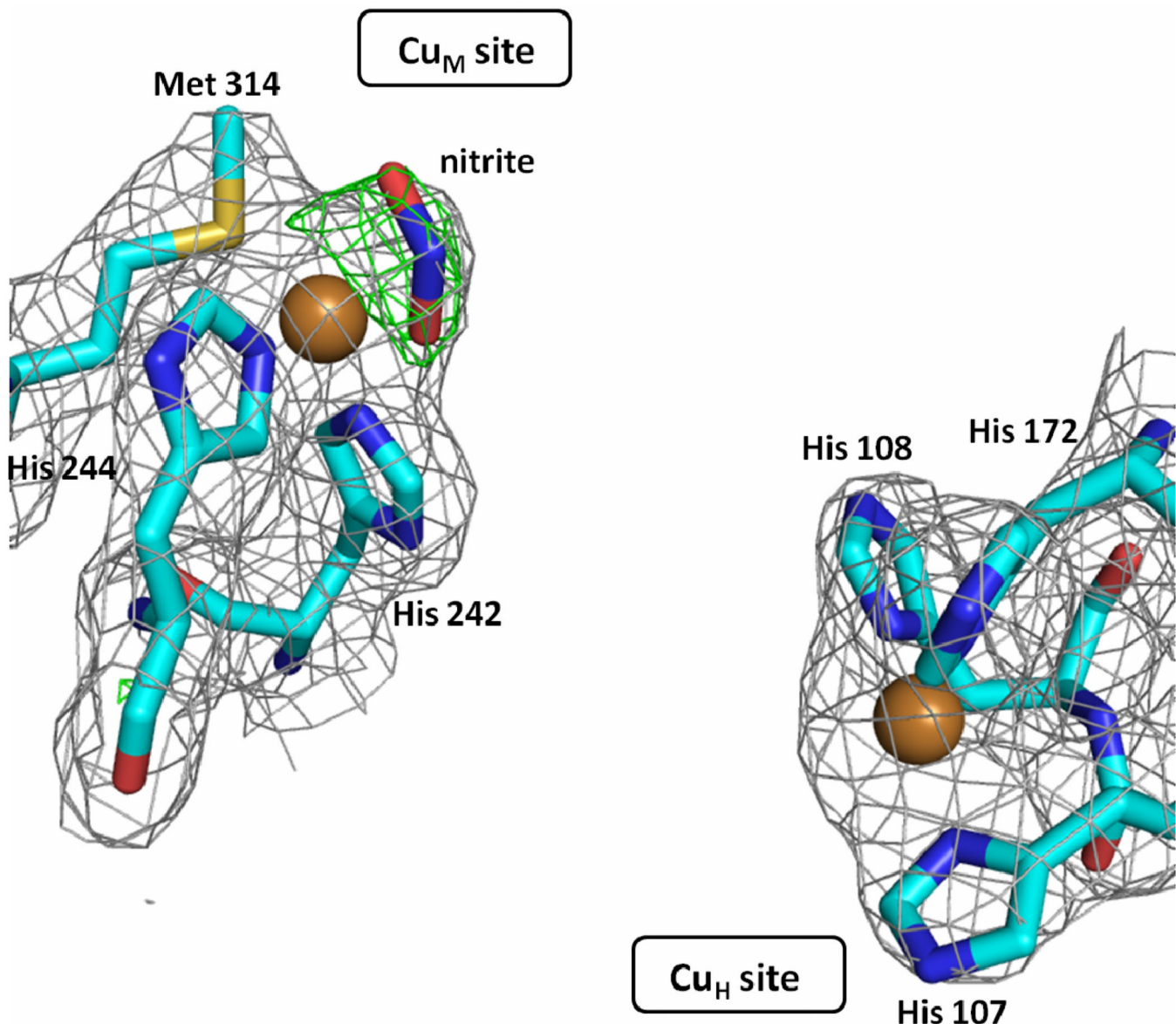


**Figure 2. The structure of Cu<sub>M</sub> and Cu<sub>H</sub> sites of a nitrite-soaked PHMcc**

The nitrite is shown bound to Cu<sub>M</sub> in an asymmetric bidentate fashion (Cu-O1 = 1.9 Å; Cu-O2 = 2.6 Å). The gray mesh shows the sigma weighted 2mFo-DFc (contoured at 1.0 σ) and the green mesh the mFo-DFc omit maps (contoured at 2.8 σ). The omit maps were computed with Refmac5. Carbons are colored cyan, nitrogens blue, oxygens red, sulphur yellow and copper gold.

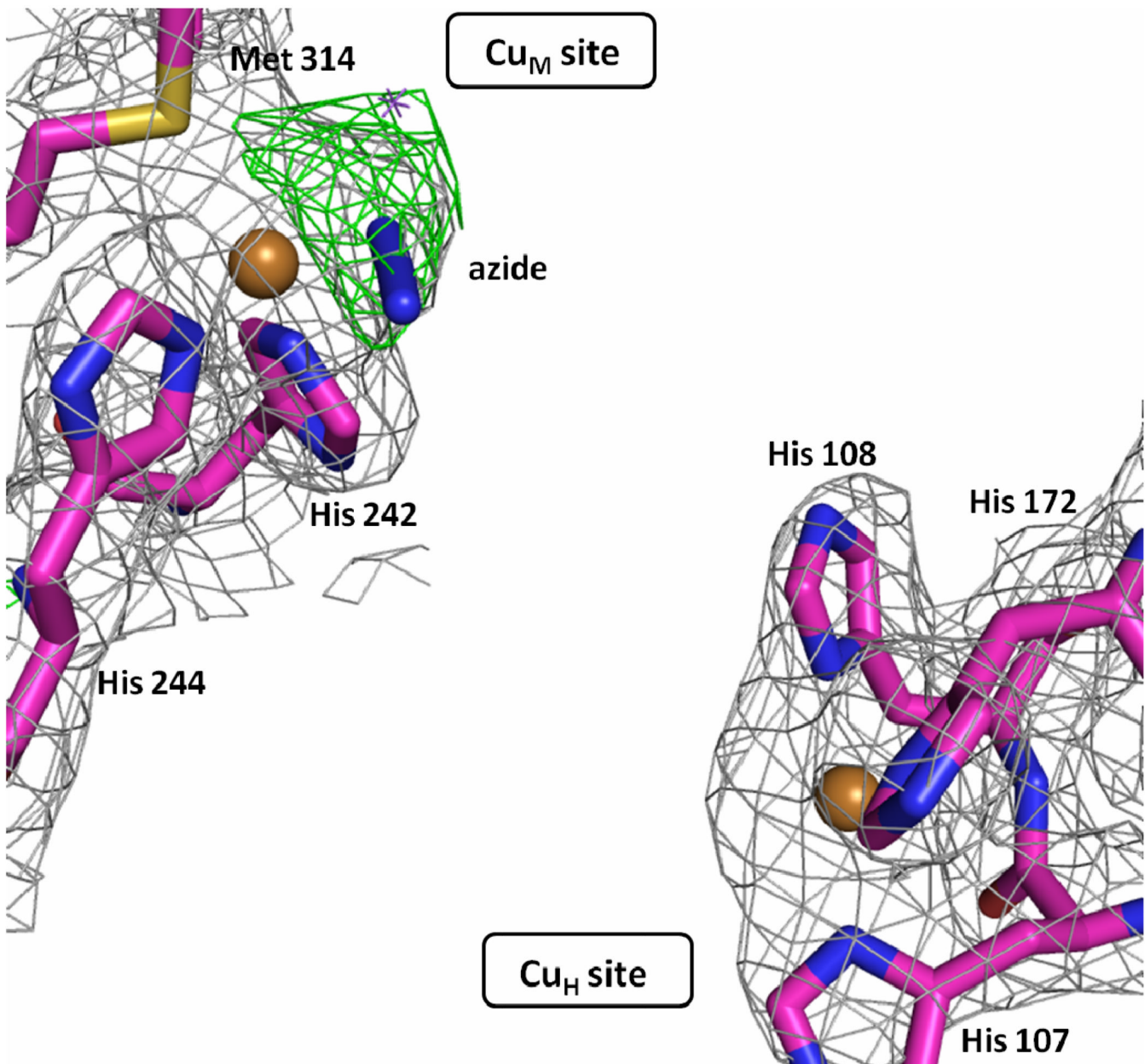


**Figure 3. Structure of  $\text{Cu}_M$  and  $\text{Cu}_H$  sites in PHMcc-azide crystals**

The azide is shown bound to  $\text{Cu}_M$  in a monodentate fashion ( $\text{Cu}-\text{N} = 2.0 \text{ \AA}$ ). The gray mesh shows the sigma weighted 2mFo-DFc (contoured at 1.0  $\sigma$ ) and the green mesh the mFo-DFc omit maps (contoured at 2.8  $\sigma$ ). The omit maps were computed with Refmac5. Carbons are colored magenta, nitrogens blue, oxygens red, sulphur yellow and copper gold.

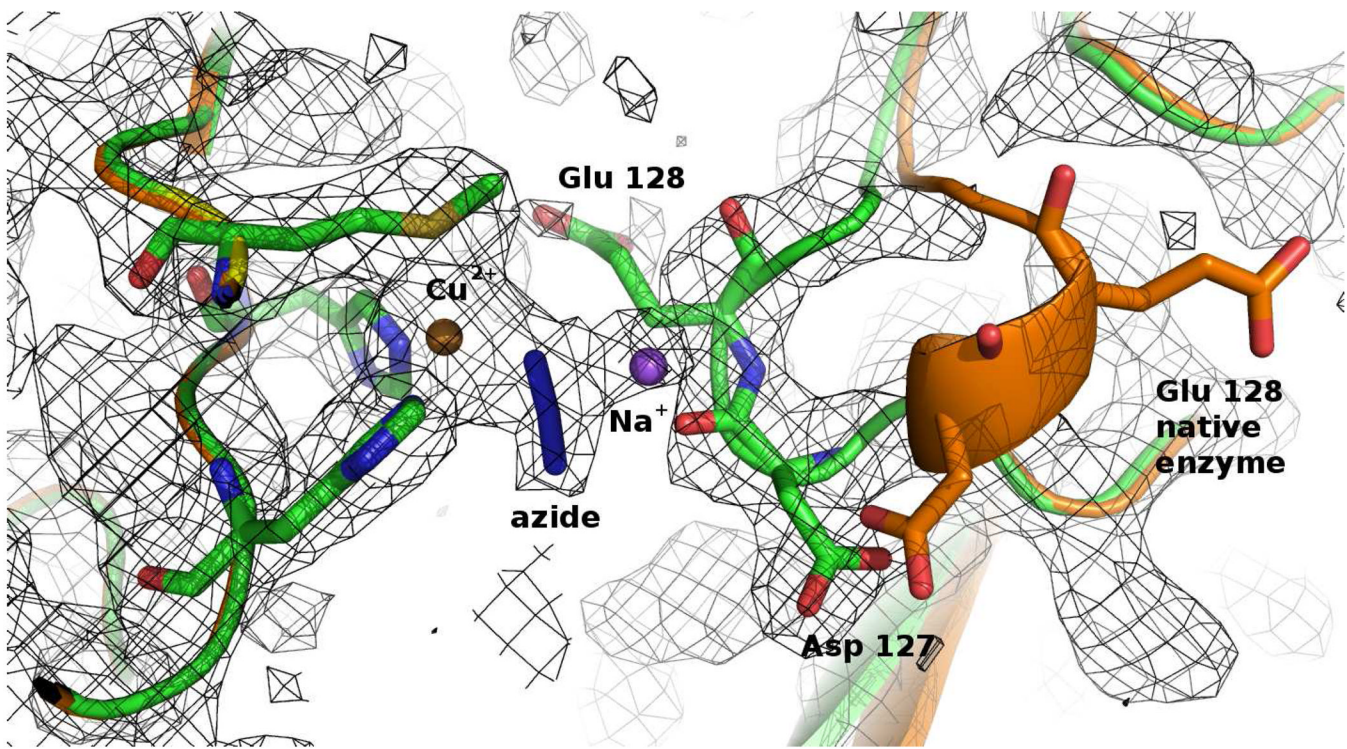


**Figure 4. The loop Asp<sup>127</sup> to Thr<sup>130</sup> is closer to the Cu<sub>M</sub> site in the PHMcc-azide than in the native enzyme**

The gray mesh represents the 2Fo-Fc electron density contoured at 1.0  $\sigma$ . Carbons are colored green, nitrogens blue, oxygens red, sulphur yellow, copper gold and sodium purple. The original position of the loop when PHM is crystallized with just 3 mM NaN<sub>3</sub> (instead of 40 mM) is shown in orange.

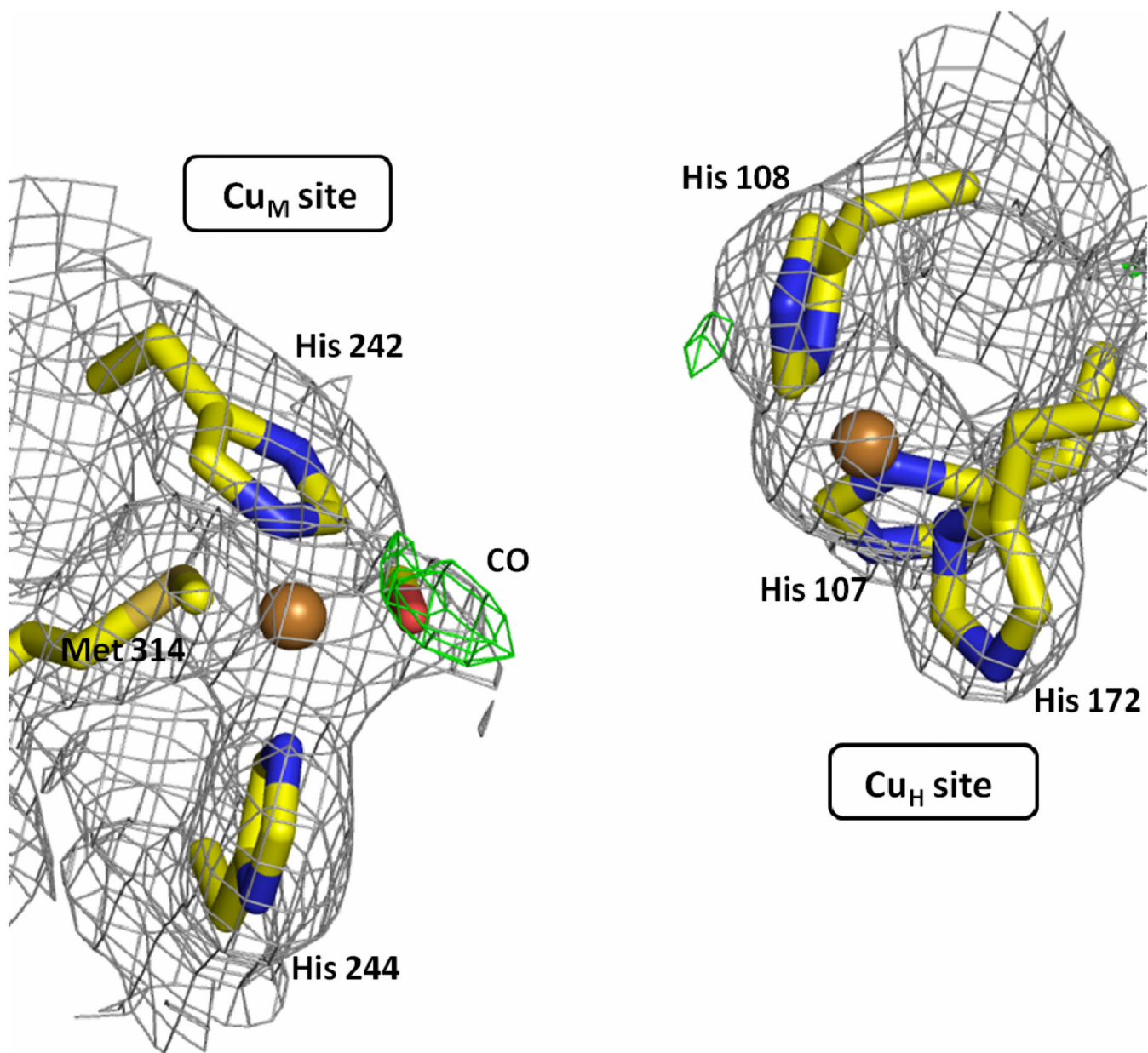
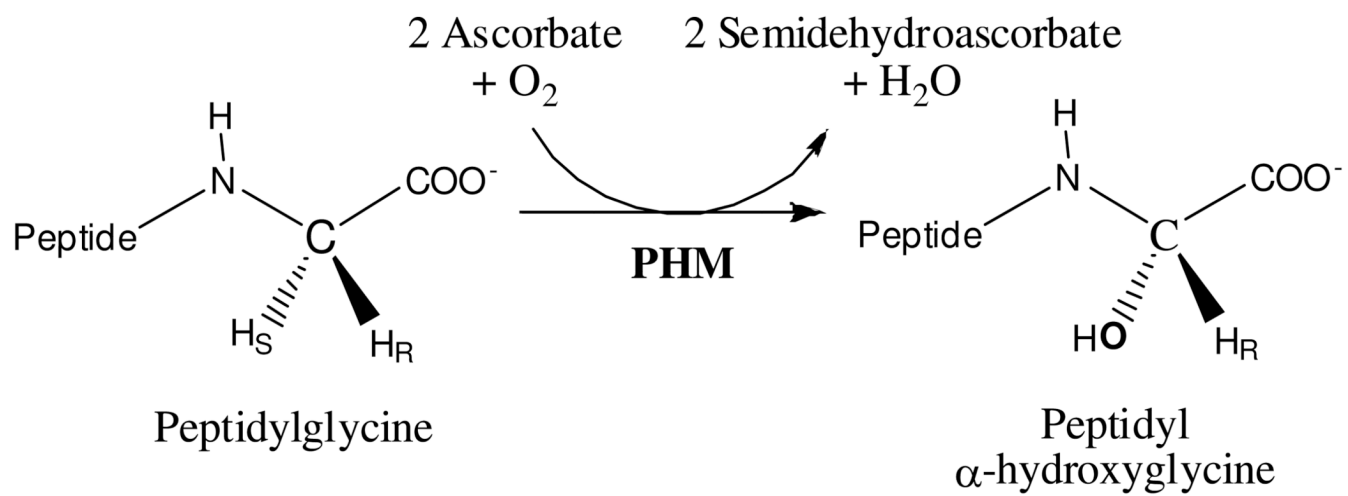


**Figure 5. The structure of Cu<sub>M</sub> and Cu<sub>H</sub> sites of the reduced-PHMcc-CO complex**  
The CO is shown bound to Cu<sub>M</sub> in a bent configuration (Cu-C = 1.8 Å; Cu-C-O = 110°). The gray mesh shows the sigma weighted 2mFo-DFc (contoured at 1.0 σ) and the green mesh the mFo-DFc omit maps (contoured at 2.8 σ). The omit maps were computed with Refmac5. Carbons are colored yellow, nitrogens blue, oxygens red, sulfur yellow-orange and copper gold.



**Scheme 1.**  
The Stereo-Specific Reaction Catalyzed by PHM

**Table 1**

Statistics for crystallographic data collection and refinement for oxidized-PHM<sub>CC</sub> complexes under different conditions

	ox-PHM <sub>CC</sub> -NO <sub>2</sub> <sup>-</sup> 300 mM 20 h soak	ox-PHM <sub>CC</sub> -N <sub>3</sub> <sup>-</sup> 40 mM Co-crystal	ox-PHM <sub>CC</sub> -N <sub>3</sub> <sup>-</sup> 100 mM 1.5 h soak	ox-PHM <sub>CC</sub> -N <sub>3</sub> <sup>-</sup> 50 mM 26 h soak	ox-PHM <sub>CC</sub> -CO 3 atm 15 min. soak	ox-PHM <sub>CC</sub> - subs-nitrite	ox-PHM <sub>CC</sub> - subs-azide
Unit cell parameters (Å)	a = 68.6 b = 68.6 c = 80.3	a = 68.5 b = 68.6 c = 81.4	a = 68.9 b = 69.3 c = 81.5	a = 68.7 b = 69.0 c = 81.3	a = 69.2 b = 69.7 c = 83.1	a = 68.4 b = 68.8 c = 80.0	a = 68.1 b = 68.8 c = 79.8
Space group	P2 <sub>1</sub> 2 <sub>1</sub> 2 <sub>1</sub>	P2 <sub>1</sub> 2 <sub>1</sub> 2 <sub>1</sub>	P2 <sub>1</sub> 2 <sub>1</sub> 2 <sub>1</sub>	P2 <sub>1</sub> 2 <sub>1</sub> 2 <sub>1</sub>	P2 <sub>1</sub> 2 <sub>1</sub> 2 <sub>1</sub>	P2 <sub>1</sub> 2 <sub>1</sub> 2 <sub>1</sub>	P2 <sub>1</sub> 2 <sub>1</sub> 2 <sub>1</sub>
Source	X6A	Rotating anode	Rotating anode	Rotating anode	X25	X4C	X4C
Wavelength (Å)	1.00	1.54	1.54	1.54	1.10	0.98	0.98
Resolution (Å)	52 – 2.35	52 – 2.40	53 – 3.05	53 – 3.25	35 – 2.00	52 – 2.70	52 – 2.75
Unique reflections	16,345	15,128	7,716	6,295	37,462	10,776	8,970
Redundancy	7.1 (6.8)	5.0 (5.1)	5.3 (5.4)	5.6 (5.8)	5.9 (6.7)	7.0 (5.6)	4.8 (3.0)
Completeness (%)	99.7 (100.0)	99.5 (99.9)	99.8 (100.0)	98.7 (99.5)	97.0 (100.0)	99.0 (91.4)	87.3 (49.3)
<1>/s<1>	49.4 (3.7)	25.2 (3.1)	22.1 (4.1)	20.9 (4.3)	4.6 (1.5)	35.7 (2.1)	21.1 (1.7)
Rsym (%)	4.6 (49)	11.1 (59)	10.0 (51)	10.3 (54)	8.0 (41)	8.5 (53)	8.9 (41)
<b>Refinement</b>							
Rcryst / Rfree (%)	20 / 24	20 / 26	20 / 25	19 / 24	21 / 24	22 / 27	24 / 30
<b>Stereochemistry</b>							
R.M.S. bond lengths (Å)	0.007	0.008	0.011	0.012	0.009	0.012	0.006
R.M.S. angles (°)	1.06	1.07	1.15	1.20	1.10	1.22	0.97
<b>Model composition</b>							
Amino acids	308	309	311	310	310	309	307
Cu / Ni / Na	2 / 1 / -	2 / 1 / 2	2 / 1 / -	2 / 1 / 1	2 / 1 / -	2 / 1 / -	2 / 1 / 4
Nitrite	3	-	-	-	-	2	-
Azide	-	2	3	3	-	-	6
CO	-	-	-	-	1	-	-
Glycerol	3	3	3	3	4	1	-
Water	168	215	16	12	163	18	18
Total atoms	2,597	2,677	2,471	2,461	2,692	2,443	2,437

	ox-PHM <sub>c</sub> -NO <sub>2</sub> 300 mM 20 h soak	ox-PHM <sub>c</sub> -N <sub>3</sub> 40 mM Co-crystal	ox-PHM <sub>c</sub> -N <sub>3</sub> 100 mM 1.5 h soak	ox-PHM <sub>c</sub> -N <sub>3</sub> 50 mM 26 h soak	ox-PHM <sub>c</sub> -CO 3 atm 15 min. soak	ox-PHM <sub>c</sub> - subs-nitrite	ox-PHM <sub>c</sub> - sub-sazide
PDB ID code	3MB	3MIC	3MID	3MIE	3MIF	3MIG	3MH

Numbers in parenthesis correspond to the last resolution shell.

**Table 2**

Statistics for crystallographic data collection and refinement for reduced-PHMcc complexes under different conditions

	reduced-PHMcc-nitrite 300 mM	reduced-PHMcc-azide 50 mM	reduced-PHMcc-CO 3 atm
Unit cell parameters (Å)	a = 69.0 b = 69.3 c = 81.1	a = 68.1 b = 69.1 c = 79.9	a = 69.2 b = 68.9 c = 81.7
Space group	P2 <sub>1</sub> 2 <sub>1</sub> 2 <sub>1</sub>	P2 <sub>1</sub> 2 <sub>1</sub> 2 <sub>1</sub>	P2 <sub>1</sub> 2 <sub>1</sub> 2 <sub>1</sub>
Source	X4C	X4C	Rotating anode
Wavelength	0.98	0.98	1.54
Resolution (Å)	53 – 3.10	52 – 3.25	53 – 2.15
Unique	7,468	6,287	21,690
Redundancy	7.0 (6.0)	5.7 (4.6)	4.5 (4.4)
Completeness (%)	99.9 (99.0)	99.1 (91.9)	98.1 (99.4)
<I>/s<I>	23.4 (2.2)	25.3 (2.2)	29.7 (2.6)
Rsym (%)	8.1 (57)	8.8 (47)	4.6 (66)
<b>Refinement</b>			
Rcryst / Rfree (%)	22 / 28	24 / 30	21 / 26
<b>Stereochemistry</b>			
R.M.S. bond lengths(Å)	0.009	0.007	0.009
R.M.S. angles (°)	1.11	1.06	1.11
<b>Model composition</b>			
Amino acids	306	304	310
Cu / Ni / Na	1 / 1 / -	1 / 1 / -	2 / 1 / -
Nitrite / Azide / CO	2 / - / -	- / 1 / -	- / - / 2
Acetate	-	-	1
Glycerol	-	-	3
Water	12	2	153
Total	2,408	2,376	2,667
PDB ID code	3MLK	3MLL	3MLJ

Numbers in parenthesis correspond to the last resolution shell.